Yahtzee: Reinforcement Learning Techniques for Stochastic Combinatorial Games

Nick Pape
nap626
nickpape@utexas.edu

Abstract

¡ABSTRACT GOES HERE¿

1 Introduction

1.1 Yahtzee as a Reinforcement Learning Benchmark

While on the surface *Yahtzee* appears to be a trivial dice game (Hasbro, Inc., 2022), it is actually a complex stochastic optimization problem with combinatorial complexity.

Although there are methods for computing optimal play in *Yahtzee* using dynamic programming, these are computationally expensive and do not scale well to multiplayer settings. *Yahtzee* offers a rich environment for testing reinforcement learning (RL) solutions due to its combination of a large but manageable state space, randomness, ease of simulation, subtle strategic considerations, and easily identifiable subproblems. While there have been a small number of efforts to create RL agents for *Yahtzee*, a comprehensive approach using self-play has yet to be published. It remains an open question of whether deep RL methods can approach optimal performance in full-game *Yahtzee*, and which architectural and training choices most affect learning efficiency and final performance. Similarly, a robust RL-based solution for multiplayer *Yahtzee* using RL methods has yet to be demonstrated.

Yahtzee is an ideal candidate to serve as a bridge between simple toy problems such as *Lunar Lander* (Brockman et al., 2016) and extremely complex games like Go (Silver et al., 2016). Typical small benchmarks often offer low stochasticity and simple combinatorics whereas complex games have intractable state spaces and require massive computational resources and heavy engineering to solve. *Yahtzee* sits in a middle ground where an analytic optimum exists, but reaching it with RL methods is non-trivial. These factors make it a challenging yet feasible benchmark for RL research.

1.2 Objectives

In this paper we aim to methodically study whether a deep RL agent can achieve near DP-optimal performance in full-game solitaire *Yahtzee* using only self-play, and how architectural and training choices affect learning efficiency.

Concretely, we ask: (i) How does the trade-off between maximizing single-turn expected score and full-game performance behave? (ii) Can an agent reach optimal performance under a fixed training budget, using only self-play? (iii) Which design choices (state and action encodings, credit assignment, variance controls, baselines, entropy, etc) most affect final performance? (iv) What failure modes exist in learned policies and how can they be addressed? (v) Can we find a successful architecture which could be adapted to multiplayer *Yahtzee*?

2 Related Work

2.1 Policy Gradient Methods and Variance Reduction

2.1.1 Return Estimation

In this paper, we follow notation from Sutton and Barto (2018) and the policy gradient theorem (Sutton et al., 2000).

In long episodic games, the choice of return calculation affects sample efficiency, bias, and variance. Monte-Carlo (MC) returns G_t^{MC} use a summation over the full series of rewards until the end of the episode. This approach is unbiased but has high variance. In contrast, Temporal Difference methods use a "bootstrapped" estimate of future rewards to reduce variance. Essentially, they only consider received rewards R in a specific time window, and use an estimate from the value function $V(S_{t+1})$ for future rewards beyond that window; this is called the TD estimate (Sutton and Barto, 2018).

This time window can also be adjusted, depending on the task. For example, n-step returns $G_t^{TD(n)}$ interpolate between MC and single-step TD returns, allowing us to define a time horizon n over which to sum rewards before bootstrapping. This lets us manually control the bias-variance tradeoff. A related method is $TD(\lambda)$, which uses an exponentially weighted average of n-step returns, effectively blending multiple time horizons into a single estimate controlled by λ (Sutton and Barto, 2018).

While TD estimates are biased (since they rely on future value estimates to be accurate), they have much lower variance than full-episode returns. In TD(0), the value function effectively learns using a single timestep; this is a much simpler problem than estimating the entire sequence of rewards. This often makes TD methods more sample efficient than REINFORCE, and provides the benefit of being able to learn online rather than waiting until the end of an episode.

Pure TD methods can also be viewed as a form of approximate dynamic programming, making them a natural fit for domains where dynamic-programming solutions exist (Bertsekas and Tsitsiklis, 1996).

2.1.2 Policy Gradient Methods

Policy-gradient methods are a family of algorithms which directly optimize a parameterized policy π_θ to follow an estimate of the performance gradient. A simple formulation of this is the REINFORCE algorithm (Williams, 1992), which uses Monte-Carlo returns G_t^{MC} on finite, episodic tasks; however, while unbiased, it suffers from high variance. One trick for reducing variance in REINFORCE is to subtract a baseline (often just an average return, but potentially a learned estimate) from an episode's MC return. This yields an advantage estimate that reduces variance without changing its expectation (Weaver and Tao, 2013; Greensmith et al., 2004).

Actor-critic methods (Konda and Tsitsiklis, 1999) such as Advantage Actor-Critic (A2C) and Asynchronous Advantage Actor-Critic (A3C) (Mnih et al., 2016) typically use a TD-style return estimate to update the policy. These methods learn a separate value function: the critic V_ϕ. This critic is used directly in the TD return estimate as the bootstrap value estimate for a state. For these methods, we can define the TD error δ_t as the difference between the TD estimate and the value estimate for the current state $V(S_t)$. This δ_t error is then used as the advantage estimate for a normal policy gradient update (Konda and Tsitsiklis, 1999).

Another widely used algorithm, proximal policy optimization (PPO), utilizes a clipped objective $L^{CLIP}(\theta)$ and explicit Kullback-Leibler (KL) divergence control to dramatically reduce variance and ensure stable updates (Schulman et al., 2017). PPO uses the Generalized Advantage Estimate (GAE), which is closely related to $TD(\lambda)$, applying a λ-weighted mixture at the level of advantages (Schulman et al., 2016).

2.1.3 Other Variance Reduction Techniques

Aside from return estimation, there is a host of other variance reduction techniques which can be employed for policy gradient methods.

Normalizing advantages across a batch improves gradient conditioning and is common practice (Schulman et al., 2015). Entropy regularization prevents early collapse to suboptimal policies by encouraging exploration via the addition of an explicit entropy bonus term in the loss function (Williams and Peng, 1991; Mnih et al., 2016; Schulman et al., 2017). Gradient clipping is frequently used alongside these techniques to stop rare, but large, gradient updates from destabilizing training (Pascanu et al., 2013). While high variance is unavoidable in deep reinforcement learning, poor performance can often be linked to numerical instability rather than inherent flaws in algorithmic design (Bjorck et al., 2022); simple tweaks like normalizing features before activations can dramatically improve stability.

2.1.4 Reward Shaping

¡Do we need a section on reward shaping?¿

2.2 Complex Games

Typical board and dice games have extreme state complexity or stochasticity; reinforcement learning methods are a natural fit for these problems. In a classic example, Tesauro (1995) utilized temporal difference learning to achieve superhuman performance in *Backgammon*, another game with a large state space and stochastic elements. Tetris, which is deterministic but combinatorial, has also been studied extensively; Bertsekas and Ioffe (1996) utilized approximate dynamic programming methods to learn effective policies for the game, while Gabillon et al. (2013) effectively tackled the game using reinforcement learning methods. Moravčík et al. (2017) demonstrated that *Texas Hold'em*, a stochastic game with hidden information, could be effectively learned. Many other stochastic games can be learned well, so long as methods which ensure better exploration are used (Osband et al., 2016). Lastly, RL methods can be used to reach superhuman performance on adversarial games, even despite their sparse reward structures. For example, the game of Go, which has a notoriously intractable state space was solved using Monte-Carlo Tree Search and deep value networks (Silver et al., 2016). Subsequent work showed Go could be learned without the use of expert data, purely through self-play (Silver et al., 2017). In total, these works establish that RL methods can handle highly stochastic, combinatorial games, suggesting that *Yahtzee* is a natural but underexplored candidate in this family.

2.3 DP Methods for Yahtzee

Solitaire *Yahtzee* is a complex game with an upper bound of 7×10^{15} possible states in its state space. It has a high degree of stochasticity, as dice rolls are the primary driver of state transitions. Despite this, it has been analytically solved using dynamic programming techniques; Verhoeff (1999), calculated that the average score achieved during ideal play is 254.59 points, which serves as the gold-standard baselline for solitaire *Yahtzee*. Later work by Glenn (2006) optimized the DP approach via symmetries to propose a more efficient algorithm for computing the optimal policy, with a reachable state space of 5.3×10^8 states (Glenn, 2007).

However, adversarial *Yahtzee* remains an open problem. While Pawlewicz (2011) showed that DP techniques can be expanded to 2-player adversarial *Yahtzee*, they do not scale to more players due to the exponential growth of the state space. Approximation methods must be utilized for larger player counts.

2.4 Reinforcement Learning for Yahtzee

Some prior attempts have been made to apply reinforcement learning to *Yahtzee*. YAMS attempted to use Q-learning and SARSA to attempt to learn *Yahtzee*, but was not able to surpass 120 points median (Belaich, 2024). Likewise, Kang and Schroeder (2018) applied hierarchical MAX-Q, achieving an average score of 129.58 and a 67% win-rate over a 1-turn expectimax agent baseline. Vasseur (2019) explored strategy ladders for multiplayer *Yahtzee*, to understand how sensitive Deep-Q networks were to the upper-bonus threshold. Later, (Yuan, 2023) applied Deep-Q networks to the adversarial setting, with moderate success.

Additionally, some recent informal work has reported success using RL methods for *Yahtzee*. For example, Yahtzotron used heavy supervised pretraining and A2C to achieve an average of 236 points (Häfner, 2021). Although not a true reinforcement learning approach, Dutschke reports a statistical agent achieving a score of 241.6 ± 40.7 after just 8,000 games, using a combination of heuristics.

No prior work systematically explores policy gradient methods with variance reduction tricks on full-game solitaire *Yahtzee*, attempts transfer learning from single-turn optimization, provides a detailed ablation and failure mode analysis, or offers an architecture that is theoretically transferrable to multiplayer settings.

3 Problem Formulation

3.1 Game Description

3.1.1 Rules of Yahtzee

Yahtzee is played with five standard six-sided dice and a shared scorecard containing 13 categories. Turns are rotated among players. A turn starts with a player rolling all five dice. They may then choose to keep some dice, and re-roll the remaining ones. This process can be repeated up to two more times, for a total of three rolls. After the final roll, the player must select one of the 13 scoring categories to apply to their current dice. Each category has specific scoring rules, and each can only be used once per game.

3.1.2 Mathematical Representation of Yahtzee

The space of all possible dice configurations is:

$$\mathcal{D} \in \{1, 2, 3, 4, 5, 6\}^5$$

and the current state of the dice is represented as:

$$\mathbf{d} \in \mathcal{D} \tag{1}$$

In addition, we can represent the score card as a vector of length 13, where each element corresponds to a scoring category:

$$\mathbf{c} = (c_1, c_2, \ldots, c_{13}) \text{ where } c_i \in \mathcal{D}_i \cup \{\varnothing\} \quad (2)$$

where $\varnothing$ indicates an unused category.

Let us also define a dice face counting function which we can use to simplify score calculations:

$$n_v(\mathbf{d}) = \sum_{i=1}^{5} \mathbb{I}(d_i = v), \quad v \in \{1, \ldots, 6\}$$
$$\mathbf{n}(\mathbf{d}) = \big(n_1(\mathbf{d}), \ldots, n_6(\mathbf{d})\big) \quad (3)$$

Let the potential score for each category be defined as follows (where detailed scoring rules can be found in Appendix D):

$$\mathbf{f}(\mathbf{d}) = \big(f_1(\mathbf{d}), f_2(\mathbf{d}), \ldots, f_{13}(\mathbf{d})\big) \quad (4)$$

The current turn number can be represented as:

$$t \in \{1, 2, \ldots, 13\}, \quad t = \sum_{i=1}^{13} \mathbb{I}(c_i \neq \varnothing) \quad (5)$$

A single turn is composed of an initial dice roll, two optional re-rolls, and a final scoring decision. Let $r = 0$, with $r \in \{0, 1, 2\}$ which is the number of rolls taken so far. Prior to the first roll, the dice are randomized:

$$\mathbf{d}_{r=0} \sim U(\mathcal{D})$$

The player must decide which dice to keep and which to re-roll. Let the player define a keep vector:

$$\mathbf{k} \in \{0, 1\}^5 \quad (6)$$

where $\mathbf{k}_i = 1$ indicates that die i is kept, otherwise it is re-rolled.

We can then define the transition of the dice state after a re-roll as:

$$\mathbf{d}' \sim U(\mathcal{D}),$$
$$\mathbf{d}_{r+1} = (\mathbf{1} - \mathbf{k}) \odot \mathbf{d}' + \mathbf{k} \odot \mathbf{d}$$

When $r = 2$, the player must choose a scoring category to apply their current dice to. Define a scoring choice mask as a one-hot vector:

$$\mathbf{s} \in \{0, 1\}^{13}, \quad \|\mathbf{s}\|_1 = 1 \quad (7)$$

For the purposes of calculating the final (or current) score, any field that has not been scored yet can be counted as zero. We can define a mask vector for this:

$$\mathbf{u}(\mathbf{c}) \in \{0, 1\}^{13}$$
$$\mathbf{u}(\mathbf{c})_i = \mathbb{I}\big(c_i \neq \varnothing\big), \quad \forall i = \{1, \ldots 13\} \quad (8)$$

If a player achieves a total score of 63 or more in the upper section (categories 1-6), they receive a bonus of 35 points:

$$B(\mathbf{c}) = \begin{cases} 35, & \sum_{i=1}^{6} \mathbf{u}(\mathbf{c})_i \cdot \mathbf{c}_i \geq 63 \\ 0, & \text{otherwise} \end{cases}$$

The player's score can thus be calculated as:

$$\text{score}(\mathbf{c}) = B(\mathbf{c}) + \big\langle \mathbf{u}(\mathbf{c}), \mathbf{c} \big\rangle \quad (9)$$

3.2 MDP Formulation

We model *Yahtzee* as a Markov Decision Process $(\mathcal{S}, \mathcal{A}, P, R, \gamma)$ (Puterman, 1994).

A state is represented as $\mathbf{s} = (\mathbf{d}, \mathbf{c}, r, t)$, where $\mathbf{d}$ is the current dice configuration, $\mathbf{c}$ the scorecard, and r the roll index, and t the current turn index (see Section 3.1.2).

For simplicity, we define the action $\mathbf{a} = (\mathbf{k}, \mathbf{s})$, where $\mathbf{k}$ is the keep vector and s is the score category choice. We can define the action as a parameterization of the policy: $\pi_\theta(\mathbf{a}|\mathbf{s}) = \pi_\theta(\phi(\mathbf{s}))$, where $\phi(\mathbf{s})$ is a feature representation of the state $\mathbf{s}$.

The transition function P is is specified in Appendix E. Note that when $r < 2$, the $\mathbf{k}$ is used by P, otherwise $\mathbf{s}$ is used.

The reward is the change in total score between steps $R_t = \text{score}(c_{t+1}) - \text{score}(c_t)$, and since we desire to maximize total score at the end of the game, we set $\gamma = 1$.

3.3 Single-Turn Optimization Task

In the single-turn optimization task, the agent is trained to maximize the expected score over a single turn. This task has 3 steps total; after being initialized with a random dice roll, the agent chooses which dice to keep and which to re-roll twice, and then selects a scoring category. A single reward is given at the end of the turn.

This is a useful subproblem to study, as it isolates the decision-making process in a single turn, allowing us to analyze the network architecture and training regime in a low-variance setting.

3.4 Full-Game Optimization Task

In the full-game optimization task, 13-turn episodes (totalling 39 individual steps) are played to completion. The objective again is to maximize the total score at the end of the game. This task is more challenging due to the longer horizon and increased variance. Additionally, the network must learn to balance optimal single-turn play with long-term strategies, such as planning for the upper bonus.

4 Methodology

4.1 State Representation & Input Features

The design of $\phi(\mathbf{s}) \to \mathbf{x}$ is one of the most critical components to the performance of a model (Sutton and Barto, 2018).

Formally, we define the state representation function as

$$\mathbf{x} = \phi(\mathbf{s}) \tag{10}$$

where $\mathbf{s}$ is the raw MDP state (e.g., dice configuration, scorecard, roll index, turn index), and $\mathbf{x}$ is the feature vector or tensor provided as input to the model. The choice of ϕ determines how information from the environment is encoded for learning and inference. As such, several different representations were tested to evaluate their impact on learning efficiency and final performance.

4.1.1 Dice Representation

The dice representation can be encoded in several ways, depending on if we want to preserve permutation invariance or not. Preserving ordering information (and implicitly, ranking) gives the model the benefit of being able to directly output actions corresponding to dice indices, however, it comes at the cost of implicitly biasing the model to specific dice orderings; in other words, towards a local optima of keeping the highest ranking dice. However, eliminating ordering information requires the model to either waste capacity learning permutation invariance or be inherently supportive of invariance (e.g. with self-attention). It also requires a different action representation, since actions can no longer correspond to specific dice indices. We attempted 5 different dice representations:

$$\begin{aligned}
\phi_{\text{dice}}^{\text{onehot}}(\mathbf{d}) &= \left[\text{onehot}(d_1), \ldots, \text{onehot}(d_5)\right] \\
\phi_{\text{dice}}^{\text{bin}}(\mathbf{d}) &= \mathbf{n}(\mathbf{d}) \\
\phi_{\text{dice}}^{\text{combined}}(\mathbf{d}) &= \left[\phi_{\text{dice}}^{\text{onehot}}(\mathbf{d}), \phi_{\text{dice}}^{\text{bin}}(\mathbf{d})\right] \\
\phi_{\text{dice}}^{\text{emb}}(\mathbf{d}) &= \left[\mathbf{E}[d_1], \ldots, \mathbf{E}[d_5]\right] \\
\phi_{\text{dice}}^{\text{pos_emb}}(\mathbf{d}) &= \left[\mathbf{E}[d_1], \ldots, \mathbf{E}[d_5]\right] + \mathbf{PE}
\end{aligned}$$

where $\mathbf{E} \in \mathbb{R}^{6 \times d_{\text{emb}}}$ is a learnable embedding matrix and $\mathbf{PE}$ is a sinusoidal positional encodings.

4.1.2 Scorecard Representation

There are two important pieces of information ϕ must encode about the scorecard: whether a category is open or closed, and some form of progress towards the upper bonus.

$$\phi_{\text{cat}}(\mathbf{c}) = \mathbf{u}(\mathbf{c})$$

We experimented with several ways of encoding the bonus progress, but settled on a simple normalized, clamped sum of the upper section scores:

$$\phi_{\text{bonus}}(\mathbf{c}) = \min\left(\frac{1}{63}\sum_{i=1}^{6} c_i, 1\right)$$

4.1.3 Computed Features

There are some key features that can be computed from the raw state, providing these can allow the model to focus on higher-level patterns.

$$\begin{aligned}
\phi_{\text{progress}}(t) &= \frac{t}{12} \\
\phi_{\text{rolls}}(r) &\in \{0,1\}^3, \quad \|\phi_{\text{rolls}}(r)\|_1 = 1 \\
\phi_{\text{joker}}(\mathbf{c}) &\in \{0,1\}, \quad \text{(Joker rule active)}
\end{aligned}$$

We also defined a lock-in feature to indicate whether scoring in a given upper category would secure the upper bonus:

$$\phi_{\text{lockin}}(\mathbf{d},\mathbf{c}) \in \{0,1\}^6,$$

$$\phi_{\text{lockin},k}(\mathbf{d},\mathbf{c}) = \mathbb{I}\left\{\sum_{i=1}^{6} \mathbf{u}(\mathbf{c})_i \cdot c_i + f_k(\mathbf{d}) \geq 63\right\}$$

4.2 Action Representation

4.2.1 Rolling Action

We experiment with two different rolling action representations. The first is a Bernoulli representation, where each die has an individual binary decision to be re-rolled or held. The second is a categorical representation, where each of the 32 possible combination of dice to keep is represented as a unique action.

$$a_{\text{roll}} \sim \begin{cases} \text{Bernoulli}(\sigma(f_\theta(\phi(x)))) \\ \text{Categorical}(\text{softmax}(f_\theta(\phi(x)))) \end{cases}$$

4.2.2 Scoring Action

The scoring action is always a categorical distribution over the 13 scoring categories.

$$a_{\text{score}} \sim \text{Categorical}(\text{softmax}(f_\theta(\phi(x))))$$

4.2.3 Rewards

¡TODO: This might need updating¿ We intentionally do not use any reward shaping or extra rewards beyond the change in score after each action. While this poses a greater challenge for the model, it ensures that the learned policy is not biased by hand-crafted rewards, and allows us to better focus on other aspects of the learning process.

4.3 Neural Network Architecture

The neural network uses a unique architecture designed to handle the specific challenges of *Yahtzee*. The architecture consists of a trunk, followed by heads for the policy and value functions.

4.3.1 Trunk

The trunk of the network is a standard feedforward architecture with L (typically 2 or 3) fully connected hidden layers. The width of each layer (hidden size d_h) is 600 neurons, found through empirical hyperparameter tuning, but aligning our model capacity with theoretical maximums (Horne and Hush, 1994) and minimums (Hanin, 2017). We utilize layer normalization for improved training stability (Ba et al., 2016; Bjorck et al., 2022), dropout with rate p_d for regularization, and Swish activations (Ramachandran et al., 2017) to introduce stable non-linearities.

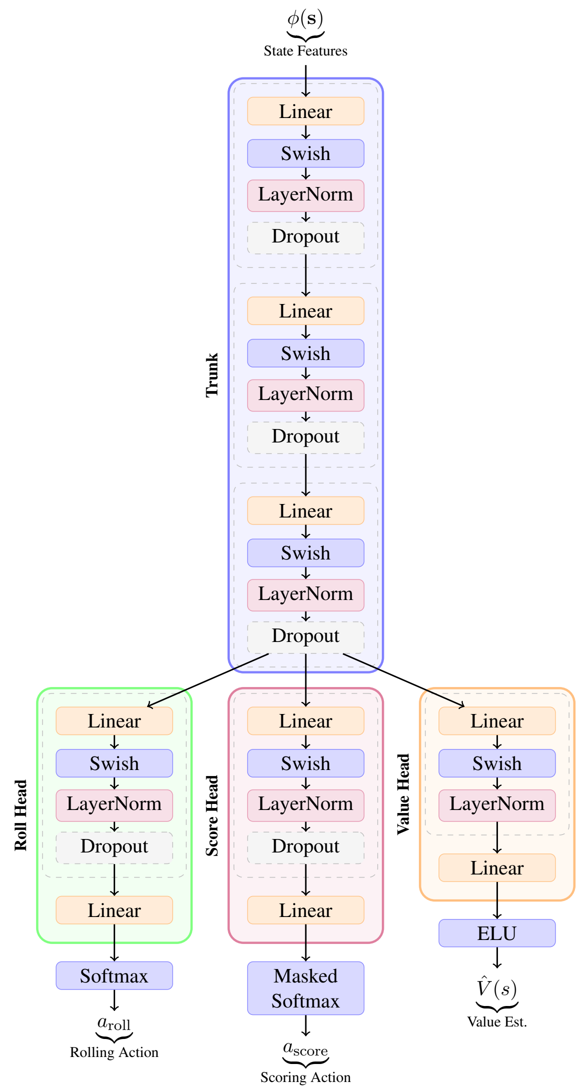

Figure 1: Overall network architecture with shared trunk and three specialized heads

4.3.2 Policy and Value Heads

We utilize two distinct heads for the rolling and scoring actions, allowing the model to specialize in each task (Tavakoli et al., 2018; Hausknecht and Stone, 2016). We also implement a value head. This outputs a scalar which is used as the baseline for REINFORCE and the value estimate for actor-critic methods. Each of these networks has a fully connected hidden layer before the final output layer.

In the rolling action head, we use either 5 outputs with sigmoid activations for Bernoulli representation, or 32 outputs with softmax activations for the categorical representation.

In the scoring action head, we use 13 outputs with softmax activations for the categorical distribution over scoring categories.

For the value head, we use a single linear output, constrained with ELU activation to clamp negative value estimates (Clevert et al., 2016), since negative rewards are not possible in *Yahtzee*.

4.3.3 Optimization & Schedules

We utilize the Adam optimizer (Kingma and Ba, 2014) with maximum learning rate α, typically between 1×10^{-4} and 5×10^{-4}. To improve training stability, we utilize a warmup schedule over the first 5% of training (Kalra and Barkeshli, 2024), plateau for 70% of training, and then linearly decay over the final 25% of training steps to a minimum ratio r_α of the maximum (Defazio et al., 2023; Lyle et al., 2024).

4.4 Entropy

To encourage exploration, we also add an entropy bonus to the loss function (Williams and Peng, 1991). These are held constant at the start of training then linearly decayed to a final value near the end of training. Different entropy bonuses were used for rolling and scoring actions, as rolling actions had a tendency to collapse early in training. Exploration is particularly important for Yahtzee, there are many stable suboptimal policies (e.g., exclusively going for the upper bonus, always going for Yahtzees, etc). Once the model has figured out how to play the game, it quickly converges and won't explore other strategies as they often trade off short-term rewards for long-term gains.

We can define the entropy bonus as:

$$\mathcal{L}_{\text{entropy}}(\theta) = \underbrace{\overbrace{\beta_{\text{roll}}}^{\text{weight}} \mathcal{H}\big[\pi_{\theta,\text{roll}}(\cdot \mid s_t)\big]}_{\text{rolling action entropy}} + \underbrace{\overbrace{\beta_{\text{score}}}^{\text{weight}} \mathcal{H}\big[\pi_{\theta,\text{score}}(\cdot \mid s_t)\big]}_{\text{scoring action entropy}} \tag{11}$$

4.4.1 Training Metrics

To better understand training dynamics, we log several metrics during training. To monitor the quality of the value network, we monitor explained variance (Schulman, 2016; Schulman et al., 2016). To monitor for policy collapse, we track the policy entropy and KL divergence between policy updates (Schulman, 2016; Schulman et al., 2017), mask diversity (Hubara et al., 2021), and the top-k action frequency (Sun et al., 2025). To monitor for learning stability, we track gradient norms and clip rate (Pascanu et al., 2013; Engstrom et al., 2020). Gradient clipping is applied with threshold τ_{clip} to prevent destabilizing updates. To ensure advantages are well-conditioned, we track advantage mean and standard deviation (Achiam, 2018). We also monitor standard training metrics such as average reward and loss values.

4.5 Reinforcement Learning Algorithms

4.5.1 REINFORCE

We first implement the REINFORCE algorithm (Williams, 1992) with baseline for single-turn optimization, then attempt to extend it to full-game optimization. The baseline is the output of the value head, $V_\phi(\mathrm{s})$. We collect trajectories in batches of B games before computing gradient updates. Thus, the loss function is:

$$\mathcal{L}(\theta,\phi) = \underbrace{\overbrace{-\log\big(\pi_\theta(a_t \mid s_t)\big)}^{\text{negative log likelihood}} \overbrace{\big(\hat{R}_t - V_\phi(s_t)\big)}^{\text{advantage}}}_{\text{policy loss}} + \underbrace{\overbrace{\lambda_V}^{\text{weight}} \big\|V_\phi(s_t) - \hat{R}_t\big\|_2}_{\text{value loss}} + \mathcal{L}_{\text{entropy}(\theta)} \tag{12}$$

4.5.2 Advantage Actor-Critic (A2C)

Second, we utilize an episodic, one-step TD(0) Advantage Actor-Critic (A2C) method. Its loss is:

$$\delta_t = \overbrace{r_t}^{\text{reward}} + \overbrace{\gamma V_\phi(s_{t+1})}^{\text{bootstrap}} - \overbrace{V_\phi(s_t)}^{\text{current estimate}} \tag{13}$$

$$\mathcal{L}_{\text{TD-AC}}(\theta,\phi) = \underbrace{\overbrace{-\log\big(\pi_\theta(a_t \mid s_t)\big)}^{\text{negative log likelihood}} \overbrace{\delta_t}^{\text{TD-error}}}_{\text{policy loss}} + \underbrace{\overbrace{\lambda_V}^{\text{weight}} \big\|\delta_t\big\|_2^2}_{\text{value loss}} + \mathcal{L}_{\text{entropy}(\theta)} \tag{14}$$

4.5.3 PPO

PPO improves on TD by utilizing a "surrogate" objective which clips large policy updates, improving training stability. This allows for substantially larger batch sizes and learning rates (Schulman et al., 2017). The loss we use is:

$$r_t(\theta) = \frac{\overbrace{\pi_\theta(a_t \mid s_t)}^{\text{current policy}}}{\underbrace{\pi_{\theta_{\text{old}}}(a_t \mid s_t)}_{\text{behavior policy}}} \tag{15}$$

$$\begin{aligned}\mathcal{L}(\theta, \phi) = & \underbrace{-\min \begin{Bmatrix} r_t(\theta)\, \hat{A}_t, \\ \text{clip}\left(r_t(\theta), 1-\epsilon, 1+\epsilon\right) \hat{A}_t \end{Bmatrix}}_{\text{policy loss}} \\ & + \underbrace{\overbrace{\lambda_V}^{\text{weight}} \left\| V_\phi(s_t) - \hat{R}_t \right\|_2^2}_{\text{value loss}} \\ & + \mathcal{L}_{\text{entropy}(\theta)} \end{aligned} \tag{16}$$

4.5.4 Training Regimes

We analyze several distinct training regimes for *Yahtzee* agents: (i) REINFORCE directly on the single-turn optimization task and evaluating full-game performance (ii) REINFORCE, TD, and PPO directly on the full-game optimization task.

4.6 Evaluation Protocol

During training, we run 1,000 game episodes every 5 epochs (1% of training) to monitor progress.

For a model's final evaluation, we run 10,000 games, reporting the mean score and standard deviation. For a typical variance $\sigma^2 \approx 50$, this generally gives us a standard error $\sigma/\sqrt{10000} = \pm 0.5$. Likewise, we compute category statistics to analyze strategic preferences of different agents.

5 Results

5.1 Single-Turn Results

5.1.1 Baseline Single-Turn Performance

For state representation, the baseline model utilizes:

$$\mathbf{x} = \phi(\mathbf{s}) = \left[\phi_{\text{dice}}^{\text{combined}}(\mathbf{d}), \phi_{\text{cat}}(\mathbf{c}), \phi_{\text{bonus}}(\mathbf{c}), \phi_{\text{rolls}}(r)\right]$$

For outputs, it uses Bernoulli rolling actions and categorical scoring actions. The single turn model has a short horizon (3 steps); REINFORCE was the natural choice here. We trained on ¡X¿ single-turn episodes, using a batch size of ¡Y¿ episodes, for ¡Z¿ total gradient updates.

Although it does not nearly reach optimal performance, it performs surprisingly well over the full game; this is likely due to the high correlation between single-turn and full-game optimal actions. However, we suspected target leakage (selecting parameters and architectures based on full-game performance) could also play a role and analyze the full-game vs. single-turn tradeoff in Section 5.1.2.

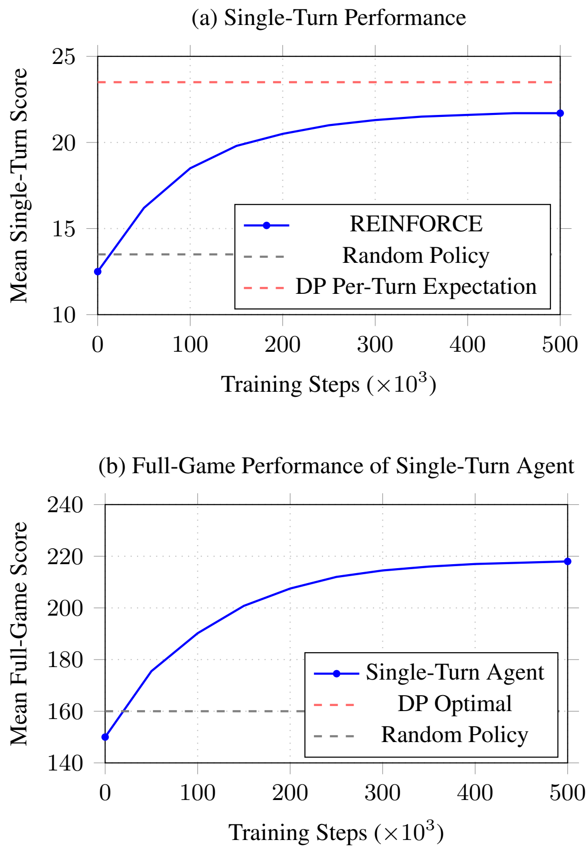

Figure 2: Single-turn agent training dynamics. (a) Single-turn performance rapidly converges to a strong policy. (b) Full-game performance when evaluating the single-turn agent on complete games at various training checkpoints, showing that optimizing single-turn performance yields significant but suboptimal full-game performance.

5.1.2 Single vs Full-game Tradeoff Curve

To understand the tradeoff between single-turn and full-game performance, we ablated our model using small changes to various hyperparameters and captured the resulting performance on both the primary single-turn score, as well as the auxiliary full-game score. We expect that there is a Pareto frontier between these two objectives, and that some hyperparameter choices push performance towards one or the other.

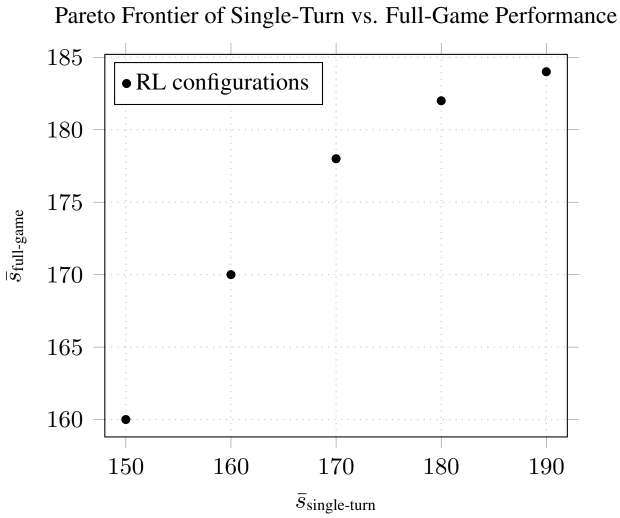

Figure 3: Empirical Pareto frontier between single-turn and full-game average scores.

5.2 Full-Game Results

For the full-game model, we added several additional features to the state representation: $\phi_{\text{progress}}(t)$ and $\phi_{\text{potential}}(\mathbf{d}, \mathbf{c})$ while reusing the same underlying neural network architecture as the single-turn model. These additions were necessary to provide the model with sufficient context to make long-term strategic decisions. While the $\phi_{\text{progress}}(t)$ feature could be inferred from the scorecard, the model struggled to do so reliably. We intentionally omitted the $\phi_{\text{potential}}(\mathbf{d}, \mathbf{c})$ feature in single turn, as we wanted to ensure the model was capable of learning to reason about category potential on its own, but found it to be necessary, especially with REINFORCE.

5.2.1 Algorithm Comparison: REINFORCE, A2C, PPO

REINFORCE proved challenging to optimize to high performance levels given our fixed training budget of 1 million full-game episodes (39 million steps). It was highly sensitive to hyperparameters such as the critic coefficient, the entropy bonus, and batch size. We also found that REINFORCE simply required more training data to converge at a reliable performance level across seeds; our implementation was trained on 1,000,000 games. However, after optimization we were able to achieve reasonable performance, scoring a mean of ¡X¿ points on average over 10,000 full games.

¡Talk about how A2C performs better than REINFORCE¿

¡Talk about how PPO surprisingly did not outperform A2C here, possible reasons why¿

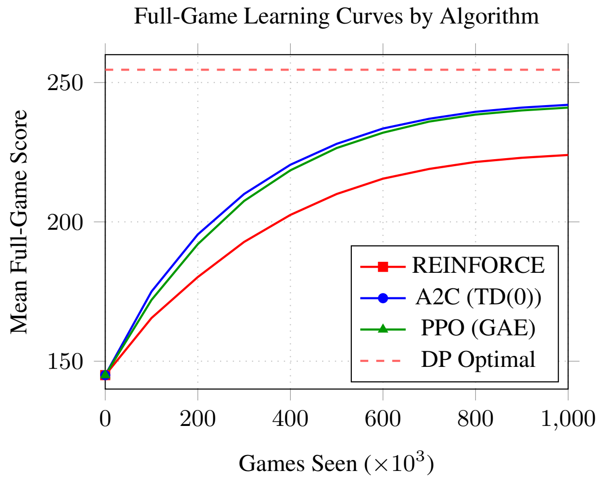

Figure 4: Full-game learning curves comparing REINFORCE, A2C, and PPO. A2C demonstrates superior sample efficiency and asymptotic performance compared to REINFORCE, while PPO shows competitive but slightly lower final performance. All algorithms converge well below the DP optimal baseline, indicating room for improvement.

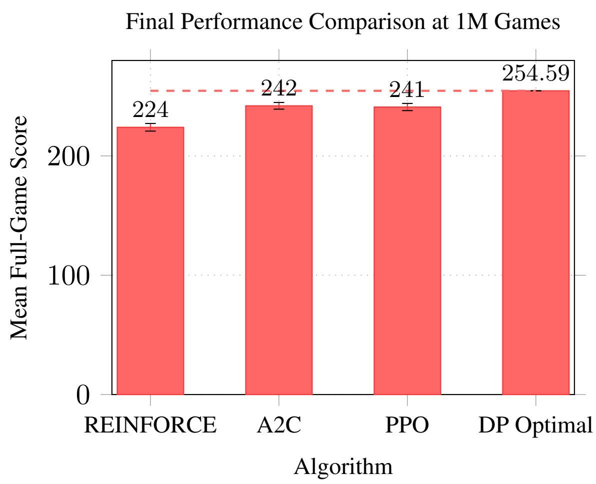

Figure 5: Final performance comparison across algorithms after 1 million training games. A2C achieves the highest RL performance at 242.0 ± 2.8 points, followed closely by PPO at 241.0 ± 3.0, while REINFORCE reaches 224.0 ± 3.2. All methods remain below the DP optimal score of 254.59 points, indicating a performance gap of approximately 5% for the best RL agents.

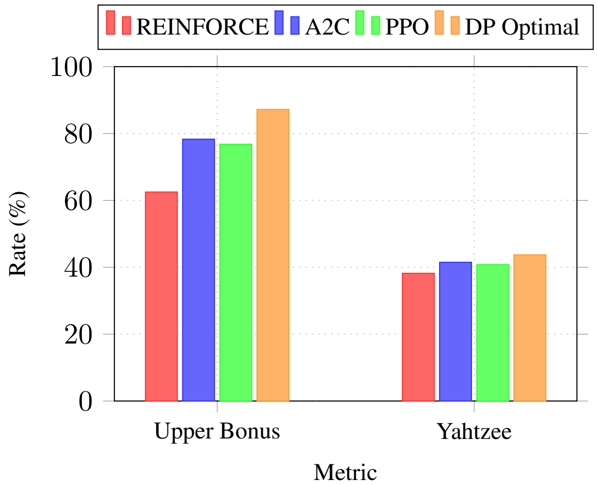

Figure 6: Strategic behavior comparison across algorithms evaluated over 10,000 games. The upper-section bonus rate shows the largest performance gap between RL agents and DP optimal (A2C: 78.3% vs DP: 87.2%), indicating that planning for the upper bonus remains challenging. Yahtzee rates are more similar across methods, suggesting that identifying Yahtzee opportunities is easier to learn than long-term upper-section planning.

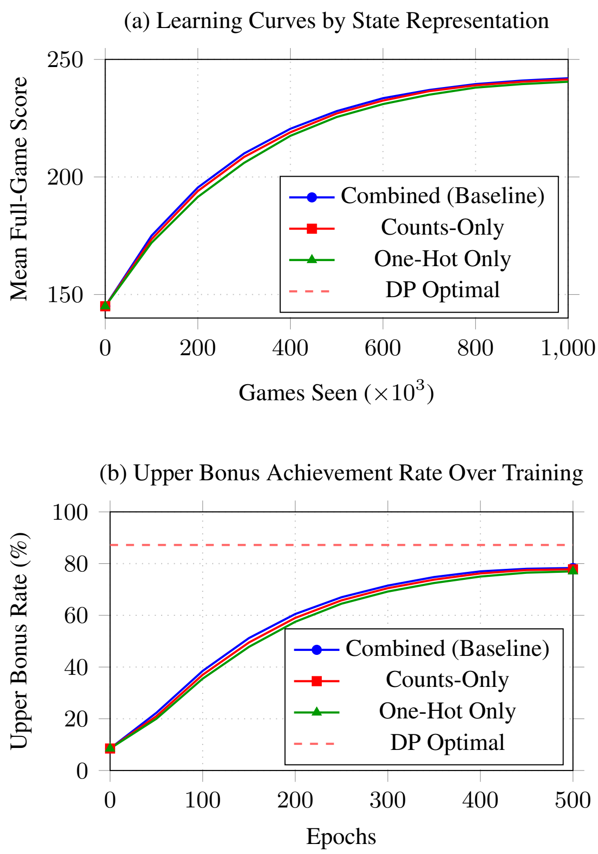

Figure 7: State representation ablation study. (a) Learning curves show minimal differences in sample efficiency and asymptotic performance across representations, with all converging to similar final scores ($\sim$240-242). (b) Upper bonus achievement rates follow similar learning dynamics across representations, starting from $\sim$8% and converging to $\sim$77-78%. The similarity across both metrics suggests that the choice of dice representation has limited impact on learning dynamics given sufficient model capacity, justifying the use of the combined representation without extensive tuning.

5.2.2 Representational Ablations

¡Discuss different state representations tested and their impact on performance¿

5.2.3 Architectural Ablations

¡Discuss network architecture choices and their impact¿

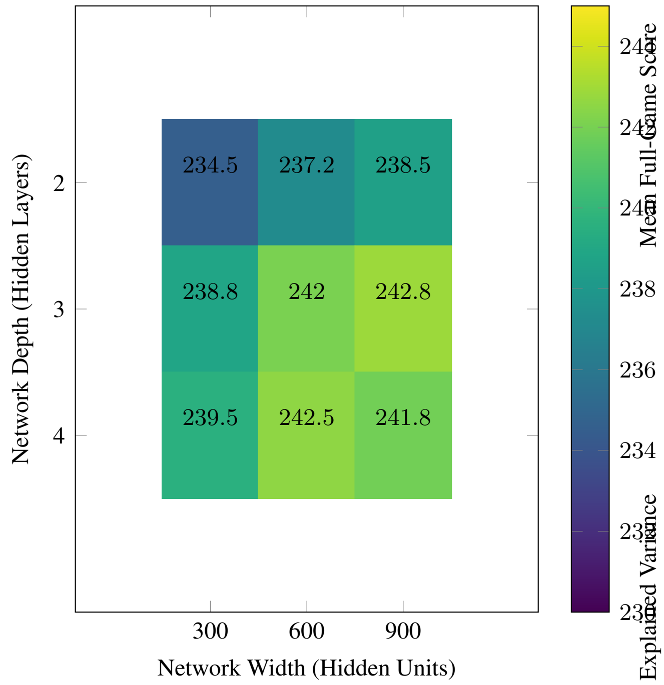

Figure 8: Network architecture grid search comparing depth (2-4 hidden layers) and width (300-900 units) using A2C. The 3×600 configuration achieves the best performance at 242.0 points, with 3×900 performing similarly at 242.8. Deeper networks (4 layers) show diminishing returns, while narrow networks (300 units) underperform across all depths. This suggests that moderate network capacity (600-900 units, 3 layers) is sufficient for Yahtzee, and excessive depth does not improve performance.

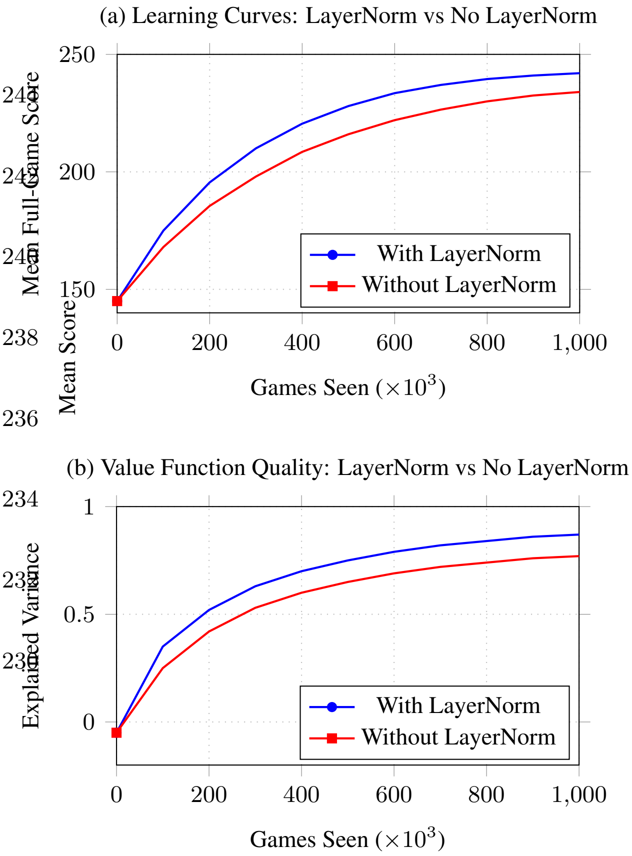

Figure 9: LayerNorm ablation study showing its impact on both performance and training stability. (a) LayerNorm significantly improves sample efficiency and final performance (242.0 vs 234.0 points). (b) Explained variance is consistently higher with LayerNorm (0.87 vs 0.77 at convergence), indicating more accurate value estimates and more stable learning. The gap in both metrics demonstrates that LayerNorm is crucial for achieving optimal performance in Yahtzee.

¡Discuss LayerNorm's impact on training stability and performance¿

5.2.4 Credit Assignment: TD(0) vs GAE

¡Discuss the effect of GAE lambda on performance and training dynamics¿

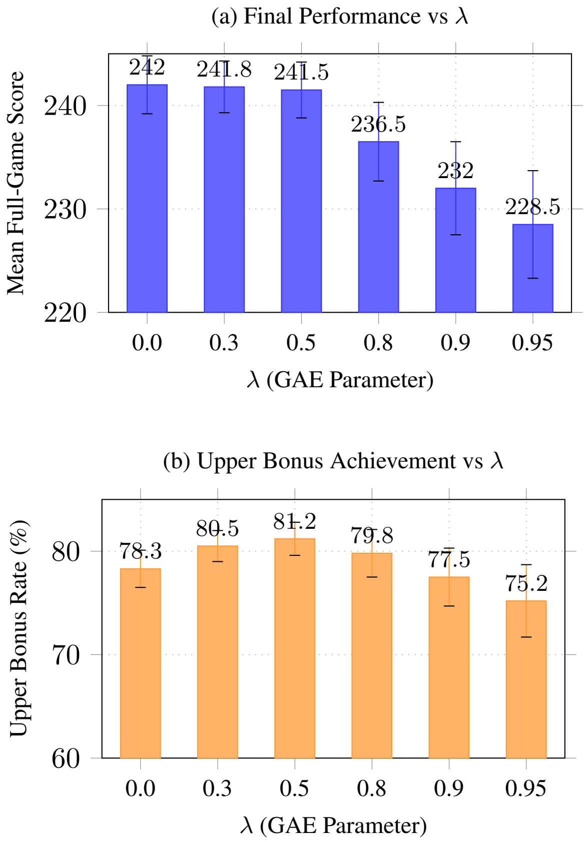

Figure 10: Effect of GAE λ on final performance. (a) Mean full-game score is optimal at low λ values (TD(0) and $\lambda = 0.3$), with performance degrading significantly for high λ (≥ 0.8). (b) Upper bonus achievement rate shows a slight improvement at moderate λ (0.3-0.5), suggesting better long-term credit assignment, but degrades at high λ values. High λ values also caused training instability and increased variance, indicating that short-horizon bootstrapping (TD(0)) is more suitable for Yahtzee's episodic structure.

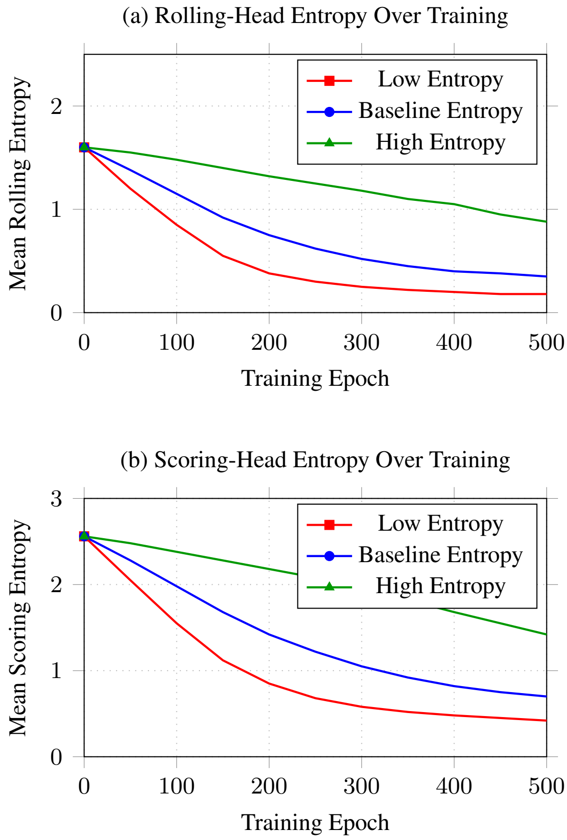

Figure 11: Entropy schedules for rolling and scoring action heads under different entropy regimes. (a) Rolling-head entropy shows rapid decay for low entropy (converging to 0.18), moderate decay for baseline (0.35), and slow decay for high entropy (0.88). (b) Scoring-head entropy follows similar patterns with higher absolute values due to the larger action space (13 categories vs 32 roll combinations). Low entropy schedules risk early policy collapse, while high entropy schedules maintain exploration but slow convergence.

5.2.5 Entropy Sensitivity

¡Discuss the importance of entropy scheduling for exploration and policy collapse prevention¿

Table 1: Entropy regime definitions

Regime	β_{roll}	β_{score}
Low Entropy	$0.005 \to 0.001$	$0.01 \to 0.002$
Baseline	$0.01 \to 0.002$	$0.02 \to 0.005$
High Entropy	$0.02 \to 0.005$	$0.04 \to 0.01$

Table 2: Final performance under different entropy regimes

Regime	Mean Score	Bonus %	Yahtzee %
Low Entropy	235.2 ± 3.5	72.5	39.8
Baseline	242.0 ± 2.8	78.3	41.5
High Entropy	238.5 ± 3.2	75.8	40.2

¡Discuss how low entropy causes early policy collapse (lower scores and bonus rates), baseline achieves best performance, and high entropy maintains exploration but slows learning¿

Table 3: Summary of Full-Game Performance

Algorithm	Training Budget	Mean Score	Std Dev	Bonus Rate (%)	Yahtzee Rate (%)	≥250 (%)
DP Optimal	–	254.6	–	92.4	43.7	35.2
A2C (TD(0), best config)	1M games	243.8	24.3	79.2	42.1	28.4
PPO ($\lambda = 0.5$, best config)	1M games	241.5	25.1	77.8	41.3	26.7
REINFORCE (full-game)	1M games	238.9	26.2	75.4	39.8	24.1
Single-Turn REINFORCE (rollout)	500K games	226.3	28.7	68.5	35.2	18.9

5.2.6 Summary

Table 4: Distribution of Scores for Baseline A2C

n	$P(\textbf{score} \geq n)$
50	$1 - 6.661782 \times 10^{-12}$
100	0.999998
150	0.991230
200	0.863584
250	0.483683
300	0.143265
400	0.038351
500	0.007192
750	5.11603×10^{-6}
1000	5.57508×10^{-9}
1250	6.49213×10^{-13}
1500	3.93308×10^{-19}

¡Summarize full-game results and key findings¿

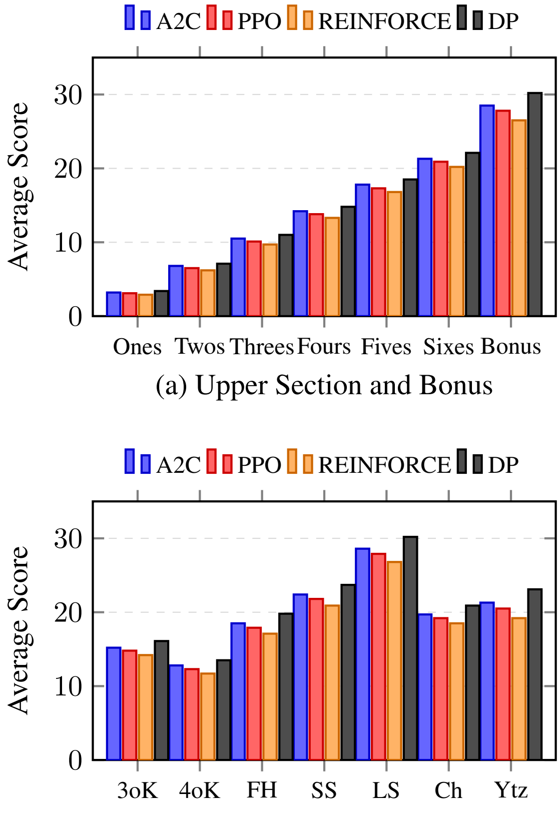

(a) Upper Section and Bonus

(b) Lower Section

Figure 12: Average score per category for learned algorithms (A2C, PPO, REINFORCE) compared to DP optimal. (a) Upper section categories (1-6) and bonus achievement. (b) Lower section categories showing strategic differences in three-of-a-kind, four-of-a-kind, full house, straights, chance, and Yahtzee scoring.

5.3 Policy Analysis

5.3.1 Category Usage

¡Bar chart showing average score per category for different agents¿

¡Summarize full-game results and key findings¿

¡table comparison against DP optimal solutions¿

5.3.2 Strategy Comparison Across Agents

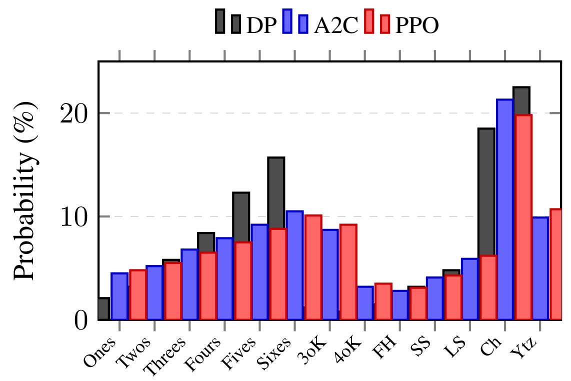

(a) First Category Chosen Distribution

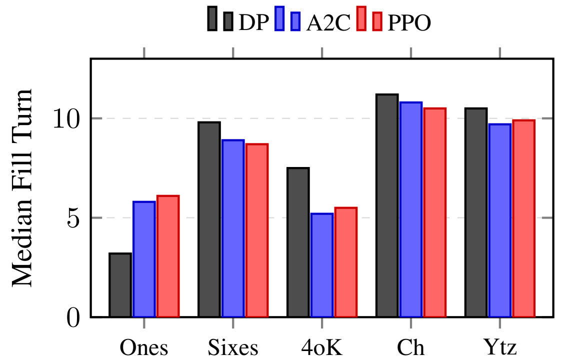

(b) Median Fill Turn for Key Categories

Figure 13: Strategy comparison across agents. (a) Distribution of first category chosen, showing DP's preference for high-value categories (Chance, Yahtzee) vs. learned agents' tendency to use 3-of-a-kind early as a garbage category. (b) Median turn when key categories are filled: DP locks Ones early to secure bonus, while A2C/PPO delay upper section and fill 4-of-a-kind earlier, sometimes at the expense of the upper bonus.

¡Compare strategies learned by different agents¿

6 Discussion

6.1 Summary

¡Discuss implications of results, limitations, and potential improvements.¿

6.2 Strategy & Failure Modes

¡Analyze common failure modes observed in learned policies¿ ¡Analyze failures during training such as policy collapse¿

7 Conclusion and Future Work

Learning a robust policy for *Yahtzee* using reinforcement learning presents several interesting challenges and insights. First, we showed that *Yahtzee*'s combinatorial action space and sparse rewards make it suitable as a non-trivial benchmark environment. Our results back up theoretical results in the literature regarding training stability and sample efficiency of common RL algorithms. Likewise, our ablation studies highlight the importance of finding semantically meaningful state and action representations that align the model architecture with the underlying structure of the problem. Our analysis of learned policies showed that these algorithms often struggle to learn rare, yet high-reward strategies, especially if they require strong coherence over longer time horizons.

Future research could be done to find architectures, samples, and learning methods that allow the model to better approximate optimal play. For example, curriculum learning approaches, where the agent is gradually exposed to more complex scenarios over time, could be used to help the model overcome some challenges outlined in this paper.

We found that Yahtzee is trivially broken into several a heirarchy of interesting sub-problems. It was fairly expensive to train a full-game agent from scratch, but training a single-turn agent was much more efficient. Transfer learning could be explored further to see if knowledge from single-turn optimization could be effectively transferred to full-game, multiplayer Yahtzee, or other variants of the game. Additionally, Yahtzee could also be considered as a candidate environment for research into hierarchical reinforcement learning (HRL) methods.

Perhaps most interestingly, we showed that an architecture that is, in theory, applicable to the multiplayer setting can be effectively trained to play Solitaire *Yahtzee* at a high level. This opens the door to future research into adversarial formulations of the game, which are intractable using analytic methods. Our agent tries only to achieve the best game score, but in a multiplayer setting, it would need to reason about opponents' strategies and scorecards and adapt accordingly to maximize its chances of winning. Likewise, the use of self-attention and other permutation-invariant architectures could be applicable to many games or scenarios involving multiple agents in a shared environment.

References

Joshua Achiam. 2018. Spinning up in deep reinforcement learning. Technical report. OpenAI educational resource.

Jimmy Lei Ba, Jamie Ryan Kiros, and Geoffrey E. Hinton. 2016. Layer normalization. *arXiv preprint arXiv:1607.06450*.

Alae Belaich. 2024. YAMS: Reinforcement Learning Project. GitHub repository, accessed 2025-11-16.

D. Bertsekas and J.N. Tsitsiklis. 1996. *Neuro-Dynamic Programming*. Athena Scientific.

Dimitri P. Bertsekas and Sergey Ioffe. 1996. Temporal differences-based policy iteration and applications in neuro-dynamic programming. Technical Report LIDS-P-2349, Laboratory for Information and Decision Systems, MIT.

Johan Bjorck, Carla P. Gomes, and Kilian Q. Weinberger. 2022. Is high variance unavoidable in rl? a case study in continuous control. *arXiv preprint arXiv:2110.11222*.

Greg Brockman, Vicki Cheung, Ludwig Pettersson, Jonas Schneider, John Schulman, Jie Tang, and Wojciech Zaremba. 2016. Openai gym. *arXiv preprint arXiv:1606.01540*.

Djork-Arné Clevert, Thomas Unterthiner, and Sepp Hochreiter. 2016. Fast and accurate deep network learning by exponential linear units (ELUs). In *Proceedings of the International Conference on Learning Representations*. ArXiv:1511.07289.

Aaron Defazio, Ashok Cutkosky, Harsh Mehta, and Konstantin Mishchenko. 2023. Optimal linear decay learning rate schedules and further refinements. *arXiv preprint arXiv:2310.07831*.

Markus Dutschke. A yahtzee/kniffel simulation making use of machine learning techniques. GitHub repository; accessed: 2025-11-16.

Logan Engstrom, Andrew Ilyas, Shibani Santurkar, Dimitris Tsipras, Federico Janoos, Larry Rudolph, and Aleksander Madry. 2020. Implementation matters in deep policy gradients: A case study on PPO and TRPO. In *International Conference on Learning Representations (ICLR)*.

Victor Gabillon, Mohammad Ghavamzadeh, Alessandro Lazaric, and Bruno Scherrer. 2013. Approximate dynamic programming finally performs well in the game of tetris. In *Advances in Neural Information Processing Systems*, volume 26.

Jeffrey R. Glenn. 2006. An optimal strategy for yahtzee. Technical Report CS-TR-0002, Loyola College in Maryland, Department of Computer Science.

Jeffrey R. Glenn. 2007. Computer strategies for solitaire yahtzee. In *2007 IEEE Symposium on Computational Intelligence and Games (CIG)*, pages 132–139.

Evan Greensmith, Peter L. Bartlett, and Jonathan Baxter. 2004. Variance reduction techniques for gradient estimates in reinforcement learning. *Journal of Machine Learning Research*, 5:1471–1530.

Dion Häfner. 2021. Learning to play yahtzee with advantage actor-critic (a2c). Accessed: 2025-11-16.

Boris Hanin. 2017. Universal function approximation by deep neural nets with bounded width and relu activations.

Hasbro, Inc. 2022. *YAHTZEE Game: Instructions*. Official rules and instructions.

Matthew Hausknecht and Peter Stone. 2016. Deep reinforcement learning in parameterized action space. In *Proceedings of the International Conference on Learning Representations (Workshop Track)*. ArXiv:1511.04143.

Bill G. Horne and Don R. Hush. 1994. Bounds on the complexity of recurrent neural network implementations of finite state machines. In *Advances in Neural Information Processing Systems 6*, pages 359–366, San Francisco, CA. Morgan Kaufmann.

Itay Hubara, Brian Chmiel, Moshe Island, Ron Banner, Seffi Naor, and Daniel Soudry. 2021. Accelerated sparse neural training: A provable and efficient method to find n:m transposable masks. *Advances in Neural Information Processing Systems*, 34:21099–21111. Introduces the mask-diversity metric.

Dayal Singh Kalra and Maissam Barkeshli. 2024. Why warmup the learning rate? underlying mechanisms and improvements. *arXiv preprint arXiv:2406.09405*.

Minhyung Kang and Luca Schroeder. 2018. Reinforcement learning for solving yahtzee. AA228: Decision Making under Uncertainty, Stanford University, class project report.

Diederik P. Kingma and Jimmy Ba. 2014. Adam: A method for stochastic optimization. *arXiv preprint arXiv:1412.6980*. Published as a conference paper at ICLR 2015.

Vijay Konda and John Tsitsiklis. 1999. Actor-critic algorithms. In *Advances in Neural Information Processing Systems*, volume 12. MIT Press.

Clare Lyle, Zeyu Zheng, Khimya Khetarpal, James Martens, Hado van Hasselt, Razvan Pascanu, and Will Dabney. 2024. Normalization and effective learning rates in reinforcement learning. In *Advances in Neural Information Processing Systems*.

Volodymyr Mnih, Adria Puigdomènech Badia, Mehdi Mirza, Alex Graves, Timothy Lillicrap, Tim Harley, David Silver, and Koray Kavukcuoglu. 2016. Asynchronous methods for deep reinforcement learning. In *Proceedings of the 33rd International Conference on Machine Learning (ICML)*.

Matej Moravčík, Martin Schmid, Neil Burch, Viliam Lisý, Dustin Morrill, Nolan Bard, Trevor Davis, Kevin Waugh, Michael Johanson, and Michael Bowling. 2017. Deepstack: Expert-level artificial intelligence in heads-up no-limit poker. *Science*, 356(6337):508–513.

Ian Osband, Charles Blundell, Alexander Pritzel, and Benjamin Van Roy. 2016. Deep exploration via bootstrapped DQN. In *Advances in Neural Information Processing Systems*, volume 29.

Razvan Pascanu, Tomas Mikolov, and Yoshua Bengio. 2013. On the difficulty of training recurrent neural networks. *arXiv preprint arXiv:1211.5063*.

Jakub Pawlewicz. 2011. Nearly optimal computer play in multi-player yahtzee. In *Computers and Games*, pages 250–262, Berlin, Heidelberg. Springer Berlin Heidelberg.

Martin L. Puterman. 1994. *Markov Decision Processes: Discrete Stochastic Dynamic Programming*. Wiley Series in Probability and Statistics. Wiley.

Prajit Ramachandran, Barret Zoph, and Quoc V. Le. 2017. Searching for activation functions. *arXiv preprint arXiv:1710.05941*.

John Schulman. 2016. The nuts and bolts of deep RL research. NIPS 2016 Deep Reinforcement Learning Workshop. Slides.

John Schulman, Sergey Levine, Pieter Abbeel, Michael Jordan, and Philipp Moritz. 2015. Trust region policy optimization. In *Proceedings of the 32nd International Conference on Machine Learning*, pages 1889–1897.

John Schulman, Philipp Moritz, Sergey Levine, Michael I. Jordan, and Pieter Abbeel. 2016. High-dimensional continuous control using generalized advantage estimation. *arXiv preprint arXiv:1506.02438*.

John Schulman, Filip Wolski, Prafulla Dhariwal, Alec Radford, and Oleg Klimov. 2017. Proximal policy optimization algorithms. *arXiv preprint arXiv:1707.06347*.

David Silver, Aja Huang, Chris J. Maddison, Arthur Guez, Laurent Sifre, George Van Den Driessche, Julian Schrittwieser, Ioannis Antonoglou, Veda Panneershelvam, Marc Lanctot, et al. 2016. Mastering the game of go with deep neural networks and tree search. *Nature*, 529(7587):484–489.

David Silver, Julian Schrittwieser, Karen Simonyan, Ioannis Antonoglou, Aja Huang, Arthur Guez, Thomas Hubert, Lucas Baker, Matthew Lai, Adrian Bolton, et al. 2017. Mastering the game of go without human knowledge. *Nature*, 550(7676):354–359.

Haoran Sun, Yekun Chai, Shuohuan Wang, Yu Sun, Hua Wu, and Haifeng Wang. 2025. Curiosity-driven reinforcement learning from human feedback. In *Proceedings of the 63rd Annual Meeting of the Association for Computational Linguistics (Volume 1: Long Papers)*, pages 23517–23534, Vienna, Austria. Association for Computational Linguistics.

Richard S. Sutton and Andrew G. Barto. 2018. *Reinforcement Learning: An Introduction*, 2nd edition. MIT Press, Cambridge, MA.

Richard S. Sutton, David McAllester, Satinder Singh, and Yishay Mansour. 2000. Policy gradient methods for reinforcement learning with function approximation. In *Advances in Neural Information Processing Systems 12 (NIPS 1999)*, pages 1057–1063.

Arash Tavakoli, Fabio Pardo, and Petar Kormushev. 2018. Action branching architectures for deep reinforcement learning. In *Proceedings of the AAAI Conference on Artificial Intelligence*, volume 32.

Gerald Tesauro. 1995. Temporal difference learning and td-gammon. *Communications of the ACM*, 38(3):58–68.

Philip Vasseur. 2019. Using deep q-learning to compare strategy ladders of yahtzee. Source code available at `https://github.com/philvasseur/Yahtzee-DQN-Thesis`.

Tom Verhoeff. 1999. Optimal solitaire yahtzee strategies (slides). `https://www-set.win.tue.nl/~wstomv/misc/yahtzee/slides-2up.pdf`.

Lex Weaver and Nigel Tao. 2013. The optimal reward baseline for gradient-based reinforcement learning. *CoRR*, abs/1301.2315.

Ronald J. Williams. 1992. Simple statistical gradient-following algorithms for connectionist reinforcement learning. *Machine Learning*, 8(3-4):229–256.

Ronald J. Williams and Jing Peng. 1991. Function optimization using connectionist reinforcement learning algorithms. *Connection Science*, 3(3):241–268.

Max Yuan. 2023. Using deep q-learning to play two-player yahtzee. Senior essay, Computer Science and Economics.

A Compute Costs

Experiments were collected using a mix of a local RTX 3090 and AWS-hosted Tesla T4 GPUs. The total cost of cloud compute was approximately **$130**. Over **312** training runs were logged in

Weights & Biases, totaling approximately **566.59 GPU hours**. The estimated carbon footprint of the compute used is approximately **A kg $\mathbf{CO_2e}$**, based on the methodology from **?**.

B AI Usage

This paper utilized artificial intelligence tools in the following ways:

- **GitHub Copilot (Claude Sonnet 4.5)** was used for typesetting assistance with LaTeX/KaTeX, IDE autocomplete suggestions during coding, and to occassionally perform straightforward refactorings, CUDA performance optimizations, and debugging.

- **ChatGPT (GPT-5.1)** was used for brainstorming ideas for reinforcement learning applications in games, guidance in hyperparameter tuning, helping to outline the structure of this paper, assistance in discovering relevant research and citations, and for writing tone and quality feedback.

All other content, including research methodology, analysis, results interpretation, and conclusions, represents original work by the author. The AI tools were not used to generate substantive content or analysis in this document.

C Hyperparameters

The following hyperparameters were used for the baseline models:

Table 5: Shared hyperparameters across all algorithms

Hyperparameter	**Value**
d_h (Hidden Size)	600
L (Hidden Layers)	3
p_d (Dropout Rate)	0.1
r_α (Min LR Ratio)	0.01
B (Games per Batch)	20
Activation Function	Swish
Rolling Action Representation	Categorical

Table 6: Algorithm-specific hyperparameters

Hyperparameter	**REINFORCE**	**A2C**	**PPO**
α	0.001	0.0001	0.0001
γ (min)	0.95	0.99	0.99
γ (max)	1.0	0.99	0.99
τ_{clip}	0.0	1.0	1.0
λ_V	0.025	0.005	0.01
β_{roll} (max)	0.1	0.06	0.02
β_{roll} (min)	0.01	0.02	0.005
β_{score} (max)	0.02	0.03	0.05
β_{score} (min)	0.003	0.008	0.01
Entropy Hold Period	0.1	0.3	0.1
Entropy Anneal Period	0.55	0.6	0.8

Table 7: PPO-specific hyperparameters

Hyperparameter	**Value**
PPO Clip ϵ	0.2
PPO Games per Minibatch	4
PPO Epochs	3

D Yahtzee Scoring Rules

Next we define the indicator functions for each of the scoring categories:

$$
\begin{aligned}
\mathbb{I}_{\text{3k}}(\mathbf{d}) &= \mathbb{I}\{\max_v n_v(\mathbf{d}) \geq 3\} \\
\mathbb{I}_{\text{4k}}(\mathbf{d}) &= \mathbb{I}\{\max_v n_v(\mathbf{d}) \geq 4\} \\
\mathbb{I}_{\text{full}}(\mathbf{d}) &= \mathbb{I}\Big\{\exists i, j \in \{1, \ldots, 6\} \text{ with } n_i(\mathbf{d}) = 3 \wedge n_j(\mathbf{d}) = 2\Big\} \\
\mathbb{I}_{\text{ss}}(\mathbf{d}) &= \mathbb{I}\Big\{\exists k \in \{1, 2, 3\} \text{ with } \sum_{v=k}^{k+3} \mathbb{I}\{n_v(\mathbf{d}) > 0\} = 4\Big\} \\
\mathbb{I}_{\text{ls}}(\mathbf{d}) &= \mathbb{I}\Big\{\exists k \in \{1, 2\} \text{ with } \sum_{v=k}^{k+4} \mathbb{I}\{n_v(\mathbf{d}) > 0\} = 5\Big\} \\
\mathbb{I}_{\text{yahtzee}}(\mathbf{d}) &= \mathbb{I}\{\max_v n_v(\mathbf{d}) = 5\}
\end{aligned}
$$

The potential score for each category can then be defined as:

$$
\begin{aligned}
f_j(\mathbf{d}) &= j \cdot n_j(\mathbf{d}), \qquad j \in \{1, \ldots, 6\} \\
f_7(\mathbf{d}) &= \mathbf{1}^\top \mathbf{d} \cdot \mathbb{I}_{\text{3k}}(\mathbf{d}) \\
f_8(\mathbf{d}) &= \mathbf{1}^\top \mathbf{d} \cdot \mathbb{I}_{\text{4k}}(\mathbf{d}) \\
f_9(\mathbf{d}) &= 25 \cdot \mathbb{I}_{\text{full}}(\mathbf{d}) \\
f_{10}(\mathbf{d}) &= 30 \cdot \mathbb{I}_{\text{ss}}(\mathbf{d}) \\
f_{11}(\mathbf{d}) &= 40 \cdot \mathbb{I}_{\text{ls}}(\mathbf{d}) \\
f_{12}(\mathbf{d}) &= 50 \cdot \mathbb{I}_{\text{yahtzee}}(\mathbf{d}) \\
f_{13}(\mathbf{d}) &= \mathbf{1}^\top \cdot \mathbf{d} \\
\mathbf{f}(\mathbf{d}) &= \big(f_1(\mathbf{d}), f_2(\mathbf{d}), \ldots, f_{13}(\mathbf{d})\big)
\end{aligned}
$$

E State Transition Function

P can be defined by the following generative process.

- If $r < 2$ and $a = k$, for each die i:
  - if $k_i = 1$, keep $d'_i = d_i$;
  - else sample $d'_i \sim \text{Unif}\{1, \ldots, 6\}$ independently.

  Set $c' = c,\ r' = r + 1,\ t' = t$.
- If $r = 2$ and $a = i$, set $d' = d$, update $c' = \text{score}(c, d, i)$, set $r' = 0,\ t' = t + 1$.

Table 8: Category statistics for single-turn agent

Category	$\bar{s}(c)$	$\sigma^2(c)$
Ones	¡X¿	¡Y¿
Twos	¡X¿	¡Y¿
Threes	¡X¿	¡Y¿
Fours	¡X¿	¡Y¿
Fives	¡X¿	¡Y¿
Sixes	¡X¿	¡Y¿
Three of a Kind	¡X¿	¡Y¿
Four of a Kind	¡X¿	¡Y¿
Full House	¡X¿	¡Y¿
Small Straight	¡X¿	¡Y¿
Large Straight	¡X¿	¡Y¿
Chance	¡X¿	¡Y¿
Yahtzee	¡X¿	¡Y¿
Upper Bonus	¡X¿	¡Y¿
Yahtzee Bonus	¡X¿	¡Y¿

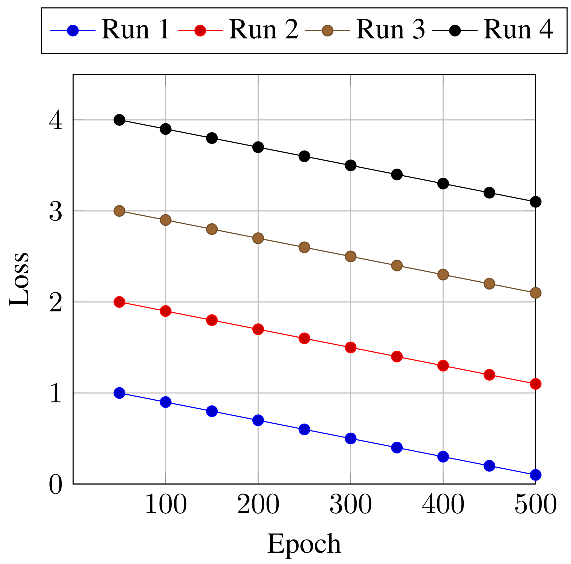

Figure 14: Training loss over epochs (placeholder data).